Nucleation and Submonolayer Growth of C_{60} on KBr

S. A. Burke,* J. M. Mativetsky, R. Hoffmann,† and P. Grütter‡
Department of Physics, McGill University, Montreal, Canada H3A 2T8
(Received 11 November 2004; published 9 March 2005)

Noncontact atomic force microscopy has been applied to the prototypical molecule-insulator system C_{60} on KBr to study nucleation and submonolayer growth. Overview images reveal an island growth mode with unusual branching structures. Simultaneous molecular and atomic resolution on the C_{60} and KBr surfaces, respectively, was obtained revealing a coincident 8×3 superstructure. Also, a 21 ± 3 pm apparent height difference was observed in atomic force microscopy topographies between some first layer molecules. One of the initial nucleation sites of the C_{60} islands was determined by observation of loosely bound molecules at kink sites in monatomic KBr steps, in conjunction with the observation that islands form preferentially at step edges.

DOI: 10.1103/PhysRevLett.94.096102 PACS numbers: 68.37.Ps, 61.46.+w, 61.48.+c, 68.43.Fg

As current semiconductor technologies reach intrinsic size limits in the nanometer range, there has been steadily growing interest in the idea of using molecules as functional building blocks for electronic devices [1]. Within this approach, one strives to exploit the characteristic electrical and optical properties exhibited by different molecular species as predetermined by their chemical identity. One additional challenge that arises, however, from this approach is that single molecules must be positioned and addressed, both for study and in a future device. This challenge can potentially be met by using scanning probe technology.

In recent years, scanning tunneling microscopy (STM) has demonstrated its ability to locally study molecules and to manipulate atoms and molecules on surfaces [2]. The study of molecular systems with STM has thus increased our general understanding of molecular growth and epitaxy on conductors as well as accelerated progress towards a molecular device. However, studies have been limited to metallic and semiconducting substrates or ultrathin insulating layers [3,4] as STM requires a conducting sample. In contrast, standard planar geometries of electronic devices require insulating substrates. As scanning force microscopy is not limited to conducting substrates, it can be applied to investigations of insulating, in addition to conducting surfaces. The development of noncontact atomic force microscopy (NC-AFM) over the past decade [5] now allows high-resolution investigation of insulating surfaces [6–9], manipulation of atoms [10], and investigations of molecules on conducting and semiconducting surfaces [11–13]. However, NC-AFM studies of molecules on insulating surfaces have still only rarely provided molecular resolution [14,15]. Most recently, atomic resolution was obtained on a single carbon nanotube with NC-AFM, showing the potential for obtaining submolecular resolution with this technique [16].

In this Letter, C_{60} on KBr(001) is considered as a prototypical molecule-insulator system. For this system, an island growth mode has been observed, similar to other molecules on alkali halides [17–19]. However, information about the initial stages of nucleation as well as the ordered molecular arrangement in ultrahigh vacuum of a free C_{60} island is still lacking. In the past, difficulties in imaging molecules on KBr(001) have arisen first because of the strong diffusion of the molecules at room temperature. Also, instabilities usually prevent imaging across step edges in NC-AFM while this is inherently important for an island growth mode [20]. While the former difficulty has recently been addressed by using a nanostructured surface and imaging a confined molecular structure [15], here we show atomic and molecular resolution at and across step edges. These results allow us to better understand the delicate balance between intermolecular forces and the weak molecule-alkali halide interactions.

All imaging was performed at room temperature using a JEOL JSPM 4500a UHV STM/AFM operated in NC-AFM mode using a NanoSurf phase-locked loop with amplitude controller for the frequency detection. A voltage was also applied between the tip and sample during imaging to minimize electrostatic forces. Highly doped *n*-type silicon cantilevers (nanosensors) with resonant frequencies of $\sim$150 kHz and spring constants of 40–50 N/m were used. Typical Q factors in UHV were $\sim$7000. The KBr crystal (Korth Kristalle, Altenholz, Germany) was introduced into the UHV system, with a base pressure less than 4×10^{-8} Pa, where the (001) surface was prepared by cleaving *in situ*, and heating for 1 h at $\sim$150 °C to remove surface charge [21]. The prepared surface was characterized by NC-AFM to verify the quality of the substrate. C_{60} molecules (Alfa Aesar 99.95% purity) were deposited on the KBr by thermal evaporation (Kentax TCE-BSC, Seelze, Germany) at 330 °C. Prior to first evaporation after introduction to UHV, the C_{60} source was outgassed at 220 °C overnight. The deposition rate was determined using a quartz crystal deposition monitor, and was 0.005 ± 0.001 ML/s.

Large scale NC-AFM images (see Fig. 1) show C_{60} islands that are generally two layers high being nucleated primarily at step edges. Islands were also observed at screw dislocation centers. The islands have an overall hexagonal

shape, although branching structures are observed in larger islands. In all cases, a mixture of some branched and some compact hexagonal crystallites were observed. The branched islands often have a two-layer structure, where the inner regions [labeled 1 in Fig. 1(d)] are ~1 nm high and have an outer rim [labeled 2 in Fig. 1(d)] that is ~2 nm high, corresponding to a single layer and a double layer of C_{60}, respectively. Preliminary experiments indicate that the islands observed are not equilibrium structures. Ongoing modeling efforts will provide further insight into the formation of these unusual island morphologies.

Where distances between steps are large, islands are also observed on terraces [see Fig. 1(d)]. The diffusion length was estimated to be ~600–800 nm at room temperature from the distance between islands on flat terraces, which is consistent with that found by Yase *et. al.* by contact-mode AFM [18]. Also, large scale images of C_{60} islands at step edges often show an alignment of one of the edges of the hexagonal islands with the ⟨100⟩ or the ⟨010⟩ direction of the KBr. However, islands found on terraces do not exhibit the same orientation with respect to the KBr, indicating that the overlayer structure is influenced by the nearby step edge, and thus different structures are expected to exist on the terraces.

High-resolution images were obtained at the edge of a C_{60} island on a KBr step, with atomic resolution on the KBr substrate and molecular resolution on the first layer of C_{60}, as shown in Fig. 2(a). Resolution of both the substrate surface structure as well as the molecular overlayer structure allows a determination of the relation between the two surfaces. In this case, a clear alignment of the high-symmetry direction, labeled b_2 in Fig. 2(b), with the ⟨100⟩ direction of the KBr is observed, and a 2:3 ratio of C_{60} molecules to KBr conventional unit cells is determined in this direction. Though a unique supercell could not be determined from the AFM topography, an evaluation of the molecular overlayer energies of the possible $n \times 3$ supercells [22] indicates that the 8×3 supercell [shown schematically in Fig. 2(b)] is the most favorable of the identified superstructures.

According to the framework proposed by Hooks *et al.* to describe epitaxy in molecular systems [24], this is a coincidence-II structure, or, as it has also been termed, geometrical coincidence. In other words, although the molecular overlayer has a long range superstructure, not all molecules lie on lattice sites or lattice lines of the substrate [24]. The molecules that sit between lattice sites, or are "out of phase" with the substrate lattice, have a higher overlayer-substrate energy. Coincident structures such as these arise frequently in molecular systems due

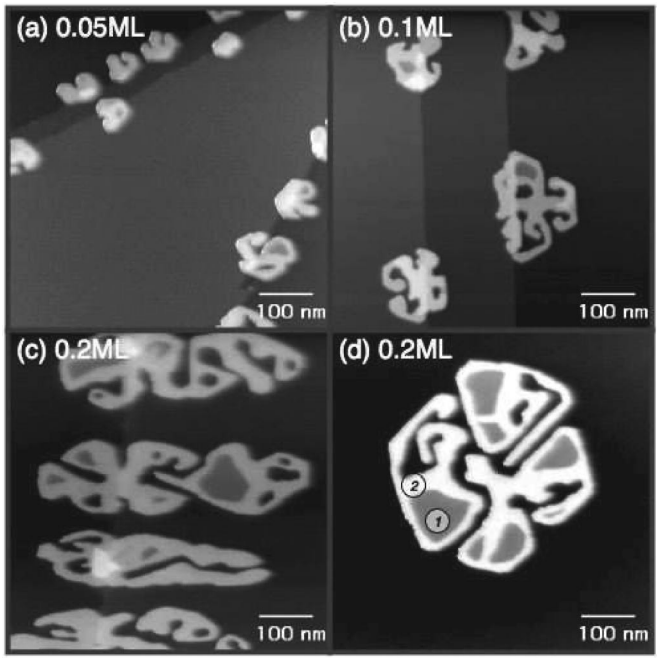

FIG. 1. Overview images, each 600 nm × 600 nm. (a) 0.05 ML C_{60}, frequency shift, $\Delta f = -3$ Hz, oscillation amplitude, $A = 7$ nm, tip-sample bias, $V_{\text{bias}} = 0.0$ V; (b) 0.1 ML C_{60}, $\Delta f = -5.6$ Hz, $A = 7$ nm, $V_{\text{bias}} = 0.8$ V; (c) 0.2 ML C_{60}, $\Delta f = -2.2$ Hz, $A = 7$ nm, $V_{\text{bias}} = -0.75$ V; (d) 0.2 ML C_{60}, $\Delta f = -2.0$ Hz, $A = 7$ nm, $V_{\text{bias}} = -0.75$ V. Region 1 is one C_{60} layer high; region 2 is two C_{60} layers high.

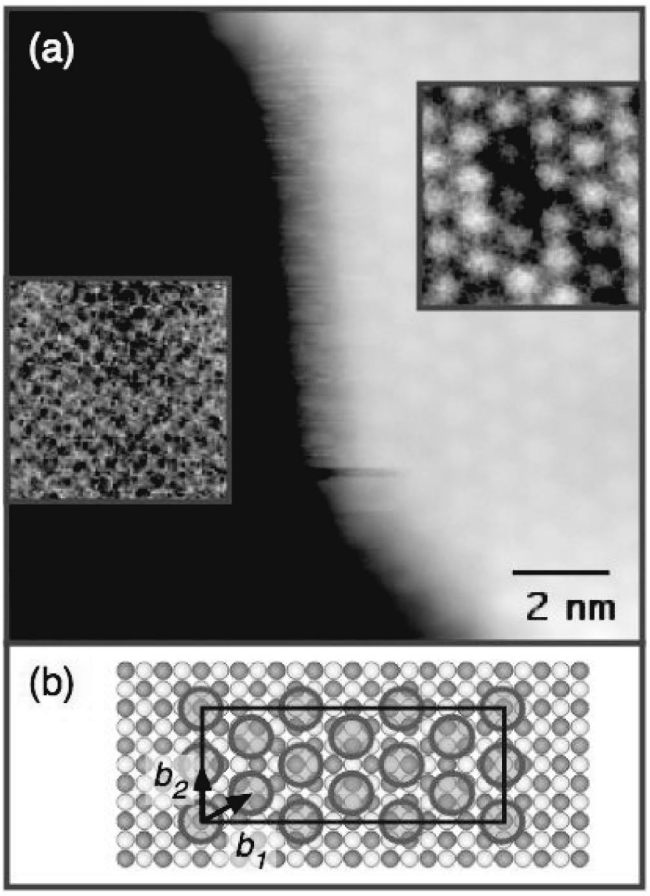

FIG. 2. Atomic/molecular resolution image of C_{60} on KBr. $\Delta f = -11.3$ Hz, $A = 7$ nm, $V_{\text{bias}} = 0.25$ V, image size: 13 nm × 13 nm. 5 nm × 5 nm insets are adjusted for contrast to show the corrugation on each surface more clearly. A schematic diagram of the 8×3 coincident structure is shown in (b).

to the interplay between the substrate-molecule interaction, the molecule-molecule interaction, and the available lattice geometries. Because of this delicate balance of interactions, a determination of the structure gives an indication of the relative energetics of the system. Previous electron diffraction studies of C_{60} thin films on alkali halides have indicated a ''weak'' epitaxial character of the molecular growth [19]. This is most likely due to the coincident epitaxy described above. Considering the 8×3 structure proposed [see Fig. 2(b)], the C_{60} overlayer remains very close to its equilibrium structure with lattice constants $b_1 = 1.010$ nm and $b_2 = 0.990$ nm with an angle of $\beta = 60.7°$ between them, compared to $b_1 = b_2 = 1.006$ nm, $\beta = 60°$ for the bulk C_{60} crystal [23]. Although other structures with fewer out-of-phase molecules may be possible, the existence of such a structure implies that the energy cost of deforming the overlayer is larger than that gained by a better fit to the lattice. This indicates a weak interaction between C_{60} and the KBr(001) surface, as does the observed island growth mode, and is consistent with temperature programmed desorption results of C_{60} on other insulating surfaces such as oxides [25].

Molecular resolution images of an area of first layer C_{60} also revealed two different effective heights in the AFM topography (see Fig. 3), giving the appearance of ''bright'' and ''dim'' molecules. The height difference between the bright and dim molecules was measured to be 21 ± 3 pm. This corresponds very closely to the geometrical height difference of 20.7 pm arising from two different orientations of a truncated icosahedron, namely, with a hexagonal ring, and pentagonal ring in contact with the surface (see inset of Fig. 3) [26]. Although AFM contrast originates in a combination of long and short range interactions which can lead to effective height differences, we believe that the geometrical height difference is the most likely explanation for the observed contrast difference. Other possible explanations include defects beneath the molecular layer and site specific reactivity. However, both of these explanations can be ruled out experimentally. The observed defect density on the KBr surface was much less than the density of dim molecules. Also, there was no clear correlation between the dim molecules and a particular underlying site of the KBr surface. In light of the interpretation proposed, it should also be noted that the first layer molecules are not rotating, or are rotating very slowly, in the out-of-plane direction, as the molecules are not observed to change contrast (i.e., from bright to dim and vice versa) over time scales of >30 min.

The phenomenon of an apparent height difference between molecules has also been observed in STM on C_{60} deposited on noble metals [27–29]. Apparent height differences observed in STM results of C_{60} on metallic substrates are 5–10 times greater [29–31] than our observations with NC-AFM on KBr. However, in STM the mechanism in these systems is somewhat different, and is attributed to an electronic difference between different orientations, or a surface reconstruction depending on the particular system [30]. On these noble metal surfaces, the C_{60} molecules have been observed to change contrast, and the frequency of this contrast change is inversely related to the strength of the interaction between the molecule and the substrate [28]. Although the lack of rotation of the first layer of C_{60} on KBr would indicate a relatively strong interaction between the molecules and the surface, it is possible that another interaction, for example, a steric hindrance, impedes the rotation.

In atomic resolution images of the KBr surface after deposition of C_{60}, small noisy patches, with an amplitude of ~ 1 nm and localized in an ~ 2 nm diameter area around kink sites at step edges, were observed (see Fig. 4). These noisy areas are also observed to disappear from one image to the next under normal imaging conditions, as shown in Fig. 4 where the region marked by the arrow returns to a ''normal'' image of a KBr kink site. The observation of such noisy, or blurred patterns is commonly associated with mobile species on the surface in STM images [32,33]. In this case, they are interpreted as one or a few

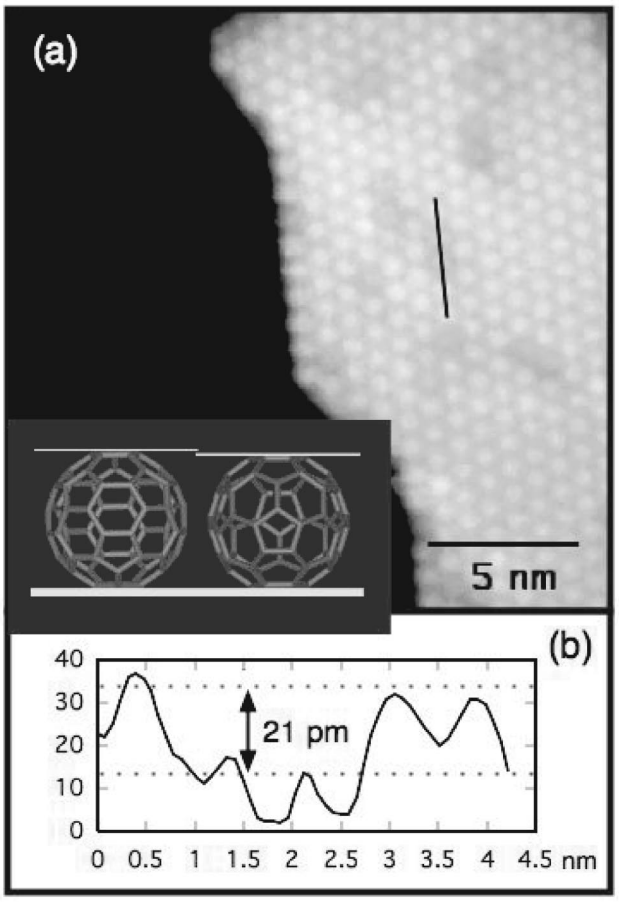

FIG. 3. (a) Molecular resolution of single layer of C_{60} shows some molecules are dim, or effectively shorter. $\Delta f = -11.3$ Hz, $A = 7$ nm, $V_{\text{bias}} = 0.25$ V, image size: 20 nm $\times$ 20 nm. (b) Cross section of image above taken at the position marked by the black line, showing the observed height difference of 21 pm. This inset image shows two orientations of the C_{60} molecule.

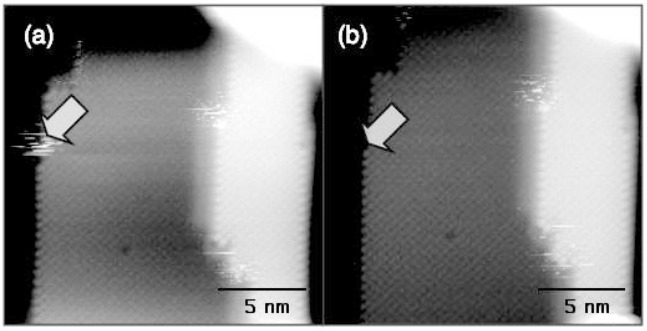

FIG. 4. Atomic resolution of KBr showing kink sites in ⟨100⟩ steps. The blurred, or noisy areas, are most likely C_{60} molecules loosely bound at the kink sites. In (b) the molecule marked by the arrow has been removed in the imaging process, revealing the underlying KBr structure. (a) $\Delta f = -7.1$ Hz, $A = 7$ nm, $V_{\text{bias}} = 0.25$ V; image size, 18 nm × 18 nm. (b) $\Delta f = -7.4$ Hz, $A = 7$ nm; image size, 18 nm × 18 nm.

C_{60} molecules which are loosely bound to the kink sites. The motion of the molecules at these sites may be caused either by thermal or tip induced motion. The relative roles of these two contributing factors is being investigated by determining the degree of localization as a function of temperature. The observation of such loosely bound C_{60} molecules at kink sites in the KBr steps, in conjunction with the observation from large scale images that islands are found predominantly at step edges, indicate that this is one of the initial nucleation sites for the C_{60} islands.

To summarize, NC-AFM was used to determine that thermally evaporated C_{60} exhibits an island growth mode on the KBr(001) surface. Additionally, the high-resolution imaging capability of NC-AFM was used to directly observe one of the initial nucleation sites and determine a coincident epitaxy of the C_{60} overlayer with the KBr substrate. The peculiar bright and dim phenomenon of C_{60} on noble metals observed by STM was also observed by NC-AFM on KBr, indicating both that the phenomenon is not specific to metallic substrates and that such differences can be observed using this technique. For molecular systems, NC-AFM can be used in a similar manner to STM to study nucleation and growth in order to better understand the surface dynamics and energetics of molecules on insulating surfaces, which have been generally inaccessible to other techniques.

We would like to thank R. Bennewitz, M. Grant, F. Rosei, and M. Stoehr for helpful discussions, as well as the following funding agencies: NSERC, CFI, NanoQuebec, FQRNT and CIAR, and the Alexander von Humboldt Foundation.

*Electronic address: burkes@physics.mcgill.ca
†Current address: Universität Karlsruhe, D-76128 Karlsruhe, Germany.
‡Electronic address: grutter@physics.mcgill.ca

[1] A. Aviram and M. A. Ratner, Chem. Phys. Lett. **29**, 277 (1974).
[2] For a recent review see, e.g., F. Rosei *et al.*, Prog. Surf. Sci. **71**, 95 (2003) and L. Pizzagalli and A. Baratoff, Phys. Rev. B **68**, 115427 (2003) and references therein.
[3] S. Schintke *et al.*, Phys. Rev. Lett. **87**, 276801 (2001).
[4] J. Repp, G. Meyer, F. Olsson, and M. Persson, Science **305**, 493 (2004).
[5] *Noncontact Atomic Force Microscopy*, edited by S. Morita, R. Wiesendanger, and E. Meyer (Springer, New York, 2002).
[6] M. Bammerlin *et al.*, Probe Microsc. **1**, 3 (1997).
[7] R. Bennewitz *et al.*, Surf. Sci. Lett. **474**, (2001).
[8] C. Barth and M. Reichling, Nature (London) **414**, 54 (2001).
[9] R. Hoffmann *et al.*, Phys. Rev. Lett. **92**, 146103 (2004).
[10] N. Oyabu *et al.*, Phys. Rev. Lett. **90**, 176102 (2003).
[11] C. Loppacher *et al.*, Phys. Rev. Lett. **90**, 066107 (2003).
[12] J. M. Mativetsky *et al.*, *NC-AFM Conference Proceedings*, edited by M. Reichling [Nanotechnology 15, S40 (2004)].
[13] U. D. Schwarz *et al.*, Phys. Rev. B **52**, 5967 (1995).
[14] H. Yamada *et al.*, Appl. Surf. Sci. **188**, 391 (2002).
[15] L. Nony *et al.*, Nano Lett. **4**, 2185 (2004).
[16] M. Ashino, A. Schwarz, T. Behnke, and R. Wiesendanger, Phys. Rev. Lett. **93**, 136101 (2004).
[17] R. Lüthi *et al.*, Science **266**, 1979 (1994).
[18] K. Yase *et al.*, Thin Solid Films **331**, 131 (1998).
[19] K. Tanigaki, S. Kuroshima, and T. Ebbensen, Thin Solid Films **257**, 154 (1995).
[20] L. Nony *et al.*, in *NC-AFM Conference Proceedings*, edited by M. Reichling [Nanotechnology 15, S91 (2004)].
[21] R. Bennewitz, M. Bammerlin, and E. Meyer, *Non-Contact Atomic Force Microscopy* (Springer, New York, 2002), Chap. 5.
[22] Overlayer energies were calculated using a harmonic approximation to the potential proposed by Girifalco [23] for nearest neighbor interactions for $n \times 3$ structures with $n = 5$, 8, 11, 13, 18, 21. The energy cost per molecule to deform the overlayer to obtain the 8×3 and $c11 \times 3$ supercells identified from the image were calculated to be 0.005 and 0.030 eV, respectively.
[23] L. A. Girifalco, J. Phys. Chem. **96**, 858 (1992).
[24] D. E. Hooks, T. Fritz, and M. D. Ward, Adv. Mater. **13**, 227 (2001).
[25] M. S. Dresselhaus, G. Dresselhaus, and P. Eklund, *Science of Fullerenes and Carbon Nanotubes* (Academic, New York, 1996).
[26] E. W. Weisstein, Truncated Icosahedron, from MathWorld – A Wolfram Web Resource, http://mathworld.wolfram.com/TruncatedIcosahdron.html.
[27] E. I. Altman and R. J. Colton, Surf. Sci. **279**, 49 (1992).
[28] E. I. Altman and R. J. Colton, Surf. Sci. **295**, 13 (1993).
[29] W. W. Pai *et al.*, Phys. Rev. B **69**, 125405 (2004).
[30] M. Grobis, X. Lu, and M. F. Crommie, Phys. Rev. B **66**, 161408 (2002).
[31] Unpublished STM results by J. M. Mativetsky and R. Hoffmann with JEOL instrument described here yielded an apparent height difference of 1.0–1.5 Å for C_{60} on Au(111), $V_{\text{bias}} = 1.0$ V, $I_t = 0.1$ nA.
[32] M. Böhringer, W.-D. Schneider, and R. Berndt, Surf. Sci. **408**, 72 (1998).
[33] S. Berner *et al.*, Chem. Phys. Lett. **348**, 175 (2001).